

High entropy alloys prepared by spark plasma sintering: Mechanical and thermal properties



Chika Oliver Ujah ^{a,b,*}, Daramy Vandi Von Kallon ^a, Victor Sunday Aigbodion ^{b,c,d}

^a Department of Mechanical and Industrial Engineering Technology, University of Johannesburg, P.O. Box 524, Johannesburg, 2006, South Africa

^b Africa Centre of Excellence for Sustainable Power and Energy Development (ACE-SPED), University of Nigeria, Nsukka, 410001, Nigeria

^c Faculty of Engineering and Built Environment, University of Johannesburg, P.O. Box 524, Johannesburg, 2006, South Africa

^d Department of Metallurgical and Materials Engineering, University of Nigeria, Nsukka, 410001, Nigeria

ARTICLE INFO

Keywords:

High entropy alloys
Mechanical property
Thermal property
Microstructure
Spark plasma sintering

ABSTRACT

Conventional alloys and superalloys are useful in engineering, automotive, aerospace and medical applications. However, some are affected by high temperature oxidation while others lose strength at elevated temperatures. So, the quest to develop a material with high thermal stability, high strength at elevated temperature and high oxidation resistance, that high entropy alloys (HEAs) were invented. They are special type of alloys produced by consolidating multiple number of elements into a single entity. Their complexity, superior properties as well as their prospective wide range of applications provoked the zeal of researchers on the topic ever since their discovery for over two decades. This work, therefore, was aimed at taking a literature study on HEAs processed by spark plasma sintering (SPS). This was because SPS has been adjudged as one of the best processing techniques in powder metallurgy. The authors analyzed brief history of HEAs and SPS; mechanical, thermal and microstructural properties of HEAs; applications, challenges, and future work of HEAs. The study was concluded by observing that HEAs actually have high potential applications in aerospace, medical, military, and marine industries. However, more research needs to be done in order to maximize their usage.

1. Introduction

Alloy can be described as a mixture of a metal (base material) and one or more additive(s) (reinforcement) which can be another metal (Cu, Al, Ni) or non-metal (Si, P, C). Pristine (unreinforced) material is reinforced with dispersed phase(s) in order to introduce a specific property or improve on existing properties [1–3]. The property of the new material (alloy or composite) is enhanced in the process as a result of the introduced phase(s). Common alloys include: bronze (Cu + Sn), brass (Cu + Zn) and steel (Fe + C). Others include ferronickel (Fe + 20–30Ni), Ti64 (Ti + 6Al + 4V), Al 6000 series (Al + Mg + Si), and etc. Properties of alloys are usually superior to the pristine material because that which is deficient in the base material is augmented by the incorporated phase [4]. Alloys can also be classified as metallic (e.g. Mg alloy), intermetallic (e.g. titanium aluminide), amorphous (e.g. vitreloy), super alloys (e.g. Ni-based) or high entropy alloys (HEAs) (multiple elements like NiCoCuMgZn [5] arranged in a definite crystal structure as shown in Fig. 1).

The scope of this study is limited to high entropy alloys. HEAs are solid solution alloys made through the aggregation of multiple metallic elements to generate single crystal microstructure like body-centered cubic (BCC), face-centered cubic (FCC), or hexagonal close-packed (HCP) lattices; or a combination of two or more phases. Sometimes, evolution of precipitates like sigma (σ), B2, Topologically close-packed (TCP) or Laves phases takes place [6]. HEAs are processed by mixing 4 or more metals, according to some authors [5] or 5 or more metals [7, 8] together followed by application of heat to form a single bulk entity with specialized properties. Since the discovery of HEAs by Yeh and Cantor in their independent researches in 2004 [7, 8], hundreds of thousands of researches have been on going on this topic; and a lot of papers have been published according to the information obtained from Scopus database. From 2013 to 20th September 28, 2023, a total of 8878 peer-reviewed journal articles (Fig. 2a) and 394 peer-reviewed review articles on HEAs (Fig. 2b) have been published in Scopus-Indexed journals. This is one out of many other journal article-indexing bodies. This clearly shows that HEAs' research is geometrically increasing as the

* Corresponding author. Department of Mechanical and Industrial Engineering Technology, University of Johannesburg, P.O. Box 524, Johannesburg, 2006, South Africa.

E-mail address: chikau@uj.ac.za (C.O. Ujah).

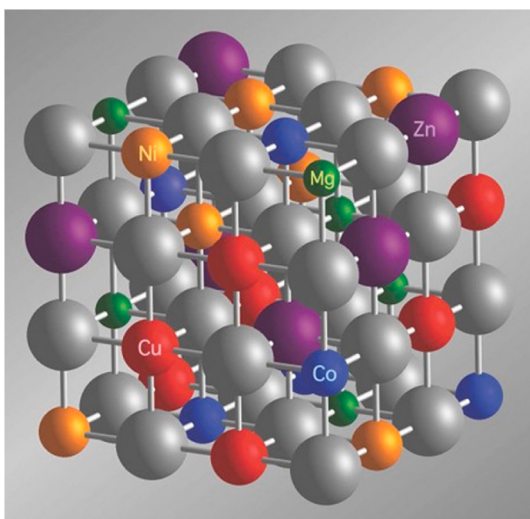


Fig. 1. Arrangement of atoms in the crystal structure of NiCoCuMgZn High Entropy Alloy [5].

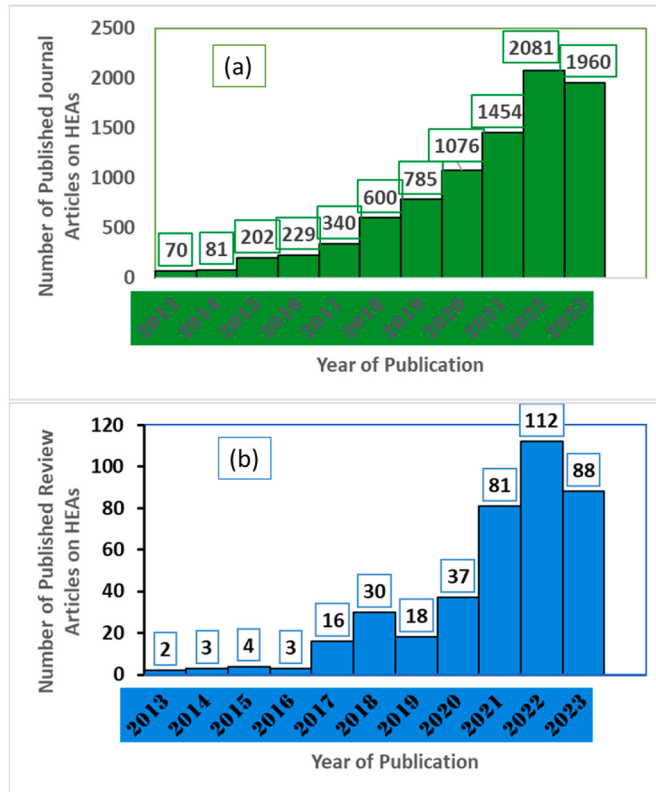


Fig. 2. Number of Scopus-Indexed Publications on HEAs from 2013 to 2024: (a) All the Scopus-Indexed Publications Excluding Conference Papers from 2013 to 2024, (b) Review Articles from 2013 to 2024 (The Data was Obtained from Scopus Data Base on September 20, 2024 and Plotted by the Authors).

year goes by. Meanwhile, review articles on HEAs are not as enormous as it ought to be considering the significance of the topic to the global technological advancement. Worse still is that works on spark plasma sintering (SPS) of HEAs are very few in the literature too. This is the precarious situation notwithstanding that a plethora of work are yet to be done on this so important topic. Hence, the aim of this study is to review latest works on the mechanical and thermal properties of SPSed HEAs in order to project the milestones that have been covered and

ascertain areas that are yet to be studied. It is through state-of-the-art reviews that the level of works covered in a topical issue can be discovered. Such review as this will keep researchers abreast of the latest discoveries in the field of discussion and get them informed of the potential areas of research that would have significant contribution to the body of knowledge in the open literature. So, properties of HEAs covered in this work were mechanical and thermal characteristics. Only these two were discussed in order to make it more comprehensive and detailed. Other properties will be treated in our next publications. Discussed further in the study included possible applications of HEAs, challenges of SPS of HEAs, future works to be done, conclusion and recommendation.

1.1. Historical background of HEAs

In 2004, there were two independently published articles by Yeh in Taiwan and Cantor in the United Kingdom where the concept of high entropy alloys (HEAs) was firstly mentioned [7–9]. Thereafter, experimental studies of this new concept escalated like a wild fire up till date as can be observed from Fig. 2. HEAs' discovery produced a tremendous landmark in the chronology of alloy development as the research has continued to grow yearly as depicted from the data available in the Scopus data base. However, the discovery of HEAs opened a new vista for Material Engineers in their quest to develop more robust materials that can outperform Ni-based, Ti-based or Al-based alloys used in aerospace components [10]. The development of such robust alloy became very imperative because the high temperature oxidation, creep and fatigue failures militate the functionality of the conventional alloys and forestall their optimal performance in some critical applications.

1.2. Spark Plasma Sintering Technique

Spark plasma sintering (SPS) can be described as a technique for consolidating powder materials by the application of pulsed direct current and axial pressure concurrently to achieve a solid bulk of the material at a very swift rate. The pulsed current generates enormous plasma heating which vaporizes impurities out of the powder mass. Hence, it is a technique that generates pure products. Reports have it that SPS accomplishes very swift consolidation via the synergistic effects of plasma and resistive heating acting simultaneously with applied axial pressure [11,12]. Sintering operation is completed at a very short time with minimum consumption of energy; the attributes which suppress grain growth and evolution of deleterious intermetallic compounds. SPS equally controls the microstructure, ensuring grain refinement and homogenous dispersion of reinforcing phase(s). The controlled microstructure promotes enhancement of the mechanical, thermal, physical and other properties of the sintered mass [13]. Besides the enormous advantages of SPS, there are some challenges that ravage the commercial viability of the technique. The limitations include: (a) It is capital intensive to install the machine; (b) it has the issue of scalability; (c) sample being sintered is not uniformly heated, and this introduces thermal gradient that leaves thermal shock to the sintered bulk. Fig. 3 shows the schematic configuration of SPS technique.

2. Properties of spark plasma sintered high entropy alloys

2.1. Mechanical properties

Going by the definition of SPS, it will be observed that the application of high temperature and pressure simultaneously induces swift densification and consolidation of powders. So, this process can produce a material with a more uniform microstructure and increased grain boundary density, thereby enhancing mechanical properties like tensile and compressive strengths, fracture toughness, stiffness and ductility [14–16]. The increase in fracture toughness of FeCoNiAlCrB alloy prepared by SPS was attributed to homogenous dispersion of boron

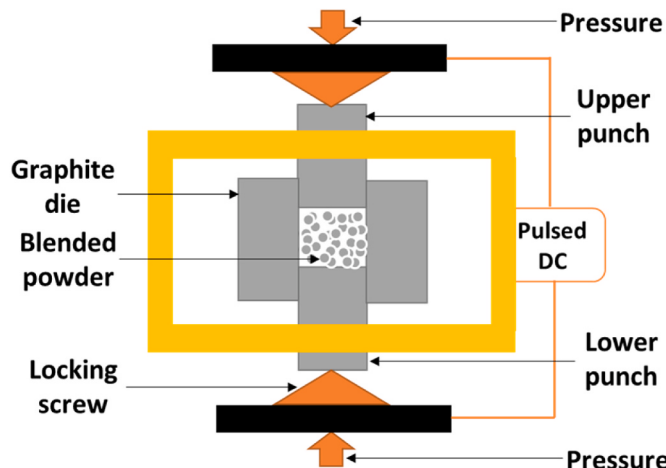


Fig. 3. Schematic illustration of spark plasma sintering technique.

reinforcement in the microstructure occasioned by the consolidation technique together with increased solid solution strengthening of boron [17]. It was reported that SPS has the propensity of grain refinement and suppression of grain growth [18]. This unique property is provoked by swift heating and cooling of the powder in the sintering chamber which ensure the enhancement of mechanical properties of HEA. Moravcik et al. [19] consolidated Ni_{1.5}Co_{1.5}CrFeTi_{0.5} with SPS technique. Results showed a bending strength of 2593 MPa, tensile strength of 1384 MPa, tensile elongation to fracture of 4.01 %, and elastic modulus of 216 GPa. These results were far much higher than results obtained from casting of the same HEA. The improvement was attributed to high grain refinement stimulated by the high mechanical-alloying propensity of the process coupled with the lattice distortion effect of HEA and oxide inclusion strengthening in the alloy. Nitrogen-doped FeMnCoCr alloy was spark plasma sintered at 900 °C, and it displayed a high compressive yield strength of 1960 MPa at room temperature which was about 7.8 times higher than that of the counterpart produced via casting; demonstrating the efficacy of SPS and N-doping in improving the compressive strength of HEAs [20]. The increase in the densification to 99.22 %, fracture toughness to 4.54 MPa·m^{1/2} and hardness to 32.3 GPa of B₄C-2vol% FeNiCoCrMo was attributed to the grain refining property of SPS, liquid phase sintering, suppression of BCC structure and formation of FCC phase [21]. It was due to grain refinement and homogenous dispersion of dispersoids [22] of SPS that consolidated Nb₄₂Mo₂₀-Ti₁₃Cr₁₂V₁₂Ta₁ exhibited highest compressive yield strength of 2680 MPa, maximum compressive strength of 3896 MPa and Vickers hardness of 741 HV at the sintering temperature of 1200 °C. These values were higher than other BCC-structured HEAs produced via casting. The efficacy of SPS in grain refinement was demonstrated in two separate studies shown in Fig. 4. It can be seen that improvement in mechanical properties of the HEA produced by SPS is far higher than that produced via vacuum arc melting (VAM) in the production of Nb₂₅Mo₂₅Ta₂₅W₂₅ alloy [23,24]. The yield stress was 132.5 % higher, the peak stress was 149 % higher while hardness and fracture strain were 74.4 % and 546 %, respectively higher; confirming the superiority of SPS over VAM.

Sun et al. [25] studied the mechanical properties of CoCrNiCuZn high entropy alloy consolidated with MA + SPS. It was observed that after mechanical alloying through ball milling for 30 h, BCC structure was the only phase observed. However, after consolidation for 700 °C, 800 °C and 900 °C consecutively, the authors realized that the highest sintering temperature gave the best mechanical characteristics: Vickers hardness of 615 HV and compressive stress of 2121 MPa. The improved mechanical strength was attributed to formation of FCC phase, grain refinement and solid solution strengthening.

More so, as the SPS technique improves the densification of consolidated composites, it conversely reduces the porosity of the material

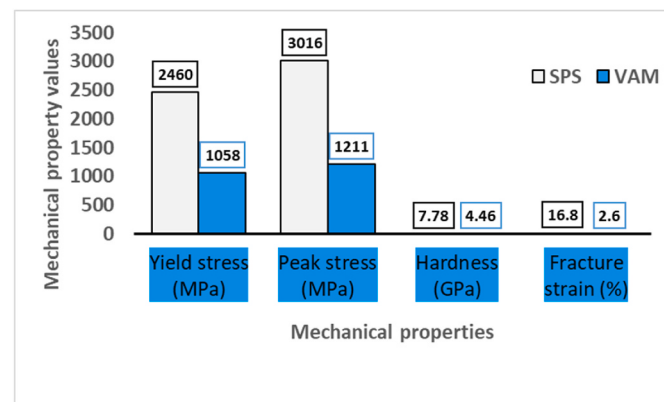


Fig. 4. Comparison of SPS and VAM (a) Peak stress and yield stress, (b) Hardness and fracture strain plots [24].

which could have been the site for growth and propagation of cracks in the fabricated components. Highly densified microstructure exhibits superior mechanical strength; while that with high porosity displays poor mechanical properties. In a study by Pan et al. [26] to characterize AlCoCrFeNi_{2.1} produced via SPS of gas-atomized powders, it was discovered that as the sintering temperature increased, the porosity got depleted, while the mechanical properties improved subsequently. The disappearance of micro pores induced improvement of both mechanical strength and ductility in the alloy, and got improved as follows: the compressive fracture strength increased to 2626.29 MPa, compressive ductility reached 45.45 %, the tensile yield strength rose to 538.13 MPa while the fracture strength became 963.55 MPa.

It has been reported that SPS can diminish the rate of segregation of constituent elements of composites or alloys; equally vaporize the impurities therein through the action of pulsed direct current thereby, improving the ductility and fracture toughness of the consolidated material. Furthermore, SPS can enhance the phase stability/transformation of HEAs by stimulating the evolution of useful phases and subduing detrimental phases. In a study involving mechanical alloying (MA) and SPS of AlCoCrFeNiSix HEA, it was observed that after MA, BCC phase was the only phase present. But after SPS, two more phases evolved, which included FCC + sigma (σ). The evolution of two more phases contributed to the enhancement of mechanical strength (hardness) of the HEA [27]. This was so because FCC phase is the ductile phase which is good at blunting and deflecting crack growth and propagation [28]. When the sintering temperature of AlCoFeMnNi-1wt%CNT HEA was increased to 900 °C, the original FCC γ -phase developed a second BCC α -phase. The evolution of dual (α + γ) structure, occasioned by the process, contributed to enhanced ultimate strength through particle strengthening and solid solution effects highlighted by the inclusion of CNTs to the alloy [29]. In another study by Yurkova et al. [30] to determine the evolution of more stable phases during SPS, it was observed that after MA, supersaturated solid solution of AlCuNiFeCr with a BCC crystalline structure only was present. But after SPS, three stable phases consisting of B2-ordered solid solution, FCC solid solution and (Fe, Cr)₂₃C₆ phases evolved. The three phases induced the increment of the Vickers hardness up to 8.51 GPa and the compressive strength up to 1960 MPa at room temperature. In comparison of TiZrNbTaMo HEA prepared through arc melting technique with that synthesized via SPS, it was observed that the microstructure of arc melted HEA was BCC single phase while that produced with SPS consisted of BCC, FCC and ZrO₂ phases. Subsequently, the measured compressive yield strengths of the arc-melted and SPSed HEA were 1390 MPa and 3759 MPa, respectively. This can only mean that SPS induced phase evolution which improved mechanical properties in HEA [31,32]. Peng et al. [33] synthesized FeCoCrNi-Mo HEA through spark plasma sintering and vacuum hot-pressing (VHP), and compared their

characteristics. The SPSed bulk composite maintained a single FCC structure while VHP precipitated three phases of σ , Mo_2C and Cr_{23}C_6 carbides. The hardness of VHP sample was higher than that of the SPS sample because the three precipitated phases in VHP sample were harder and more brittle than the FCC phase in SPSed sample. However, SPS sample enjoyed higher fracture toughness and flexural strength than VHP sample.

The fast heating and cooling rates exhibited by SPS can result to reduced number and size of precipitates which automatically translates to improved plastic deformation like increased elongation and reduced strain hardening. Microstructural study of the alloys frequently shows the evolution of nano-precipitates and eutectoid-like decompositions. Such evolutions influence the mechanical characteristics of the HEAs, like the creep, tensile strength, compressive strength, nano hardness, Vickers hardness, stiffness, fracture toughness and wear resistance [34]. The presence of micro voids and collapsing of protruded grains have been reported as some of the principal causes of mechanical depreciation in SPSed HEAs. Wang et al. [35] observed the presence of groove when CoCrFeNiMn was subjected to high strain causing uneven plastic deformation. This was initiated by the collapse of the grains followed by thermal softening. The micro voids formed on the grain boundaries buckled at high strain rate and their recombination induced cracks. In a study by Mohaty et al. [36], a rectilinear rise in Vickers hardness was observed when the sintering temperature was increased in AlCoCrFeNi HEA. The improvement could not be attributed to the relative density of the sintered sample. Samples sintered at elevated temperatures developed twin boundaries which made dislocation deformation almost impossible. Lee et al. [37] investigated the effects of Si addition to FeCoNiAl HEA produced via ball milling and SPS. The FeCoNiAlSi_x HEA ball milled powder showed only BCC phase. But when it was consolidated with SPS, there was evolution of dual phase-BCC + FCC. However, when Si was introduced into the HEA, the FCC changed into single phase BCC. The micro hardness of FeCoNiAl was 524 HV whereas that of $\text{FeCoNiAlSi}_{0.8}$ HEA was 798 HV; the maximum compressive strength of FeCoNiAl and $\text{FeCoNiAlSi}_{0.8}$ were 1325 MPa and 2031 MPa, respectively, indicating the significance of Si addition to the HEA. It was concluded that HEAs with Si was good for development of high strength structural HEAs good for automotive use. Meanwhile, when the same HEA was produced via pressureless sintering, there was poor densification which resulted in pore formation. It was recommended that the sintering must be at higher temperature and longer time for a better result [38]. In another study, it was observed that addition of 0.25 M ratio of Cu into $\text{AlFeMnTiSi}_{0.75}$ prepared by SPS yielded high hardness of 19.2 GPa and elastic modulus of 336 GPa [39]. Moreover, when the percentage weight of HfO_2 in CoCrFeMnNi HEA processed by powder metallurgy was increased from 0 to 3, the Vickers hardness got elevated from 270 ± 10 to 520 ± 10 HV, and the compressive yield strength rose from 370 MPa to 1500 MPa. Thus, attributing the improvement to grain boundary and dispersion strengthening [40]. Sharma et al. [41] worked on the microstructure and mechanical properties of non-Cantor AlCu-SiZnFe HEA produced via MA for 45 h and SPS at 600–700 °C. High energy ball milling (HEBM) evoked the formation of mostly FCC phases with traces of BCC phase. However, SPS at 600 °C did not produce high alloying and densification. It was at 650 °C that maximum mechanical properties evolved. Optimal micro hardness of 974 MPa, compressive strength of 1987 MPa and strain which increased from 11 % to 19 % were obtained at 650 °C as a result of increased formation of BCC structure. But as the sintering temperature was increased to 700 °C, the mechanical strength decreased because more FCC phase evolved.

Combination of experimental analysis and modeling in the study of HEAs has been undertaken by a number of researchers to improve the precision of findings generated. For instance, Dewangan et al. [42] investigated the creep property of HEA containing tungsten with artificial neural network (ANN) equipped with Levenberg–Marquardt algorithm. The authors observed that addition of W to HEAs led to decrement of sigma phase in the microstructure, and increased creep

resistance of the alloy. It was equally observed that predicting the creep with ANN technique gave great consistency of 0.999 % with the experimental result, confirming that the route could be useful in process and product development. Nagarjuna et al. [43] equally combined experimental analysis and ANN to study crystallite size (CS) and lattice strain (LS) of milled HEAs. It was observed that when the milling time was raised from 0 to 240 min, the CS diminished from 39.7 to 6.56 nm, while the LS improved from 0.25 % to 1.48 %. However, the ANN simulation was able to predict the CS by 96.25 % and LS by 93.43 %, confirming the reliability of the ANN. Summary of mechanical properties of most recently (not earlier than 5 years) produced and published HEAs sourced from Scopus data base are presented in Fig. 5.

Comparative analysis of the properties of HEAs and conventional alloys shows that there is a wide difference between them. Take for instance, in a comparative study between HEAs and conventional alloys, it was observed that $\text{Ti}_{36}\text{-Al}_{16}\text{-V}_{16}\text{-Fe}_{16}\text{-Cr}_{16}$ possessed Vickers hardness that is 136 % higher than that of Ti6Al4V alloy; and wear rate that is 157 % and 614 % lower than Inconel 718 alloy and TiAl alloy, respectively [44]. Table 1 shows comprehensive comparison of HEAs and conventional alloys.

2.2. Thermal properties

High entropy alloys generally possess considerable thermal conductivity, low coefficient of thermal expansion, low specific heat capacity, and averagely good thermal diffusivity. Movement of electrons in HEAs is distorted by the amalgamation of multiple elements resulting to lattice distortion. Even though, it is not appropriate to take into consideration only the role of electrons in the conduction of heat in HEAs because there are other heat carriers like phonons, photons and magnons [70,71]. Thermal conductivity is ideally a function of electrical conductivity and temperature following Weideman-Franz's law [72]:

$$k_e = L_0 \sigma T \quad (1)$$

where k_e is electronic thermal conductivity, L_0 is the Lorentz constant and takes the value of $2.45 \times 10^8 \text{ W}\Omega/\text{K}^2$, σ is the electrical conductivity and T is the temperature. In a study to determine the thermal conductivity, k comprising electron thermal conductivity k_e , and phonon thermal conductivity, k_p (since it was not magnetically ordered as to include magnon), of $\text{Al}_{0.3}\text{CoCrFeNi}$ HEA over a temperature range of 300–1100 K, it was observed that the two components of k decreased with temperature as shown in Fig. 6 [73]. The authors reported that electron thermal conductivity k_e was due to electron contribution from metals. And the impact of k_p to k in the HEA cannot be ignored because the ratio (k_p/k_e) ranged from 1.853 to 3.905, which was far much bigger than what is obtainable in traditional metals. This was why Chou et al. [74] described $\text{Al}_x\text{CoCrFeNi}$ HEA as semi-metals. The decrease in the ratio of k_p/k_e with increasing temperature points to the fact that the impact of electron thermal conductivity increased with increasing temperature, and that phonon thermal conductivity, k_p is a key player in thermal conduction of HEAs too. From Fig. 6, it will be observed that the thermal conductivity of HEA dwindled with the rise of temperature from 300 K to 1100 K, giving a weak temperature dependence of $T^{-0.47}$. The k , which is the sum of k_e and k_p , varied from 5.989 to 3.144 W/(m·K), which is 1–2 orders of magnitude lesser than that of traditional metals like Al (205 W/(m·K); Fe (46 W/(m·K); Cu (400 W/m. K) and Mg (156 W/m. K). It has been shown that heat conduction in HEAs is made up of k_p and k_e , majorly. As can be seen from Fig. 5, k_e is lower than k_p because movement of electrons is distorted in the crystal due to the differences in free-electron consistency of the different elements making up the HEA.

But k_p depends more on vibration and agitation of phonons which can jump over point defects and misaligned atoms in the crystals structure of HEAs. In the other hand, thermal expansion coefficients (TEC) of the $\text{Al}_x\text{CoCrFeNi}$ HEAs was reported. It ranges from $8.84 \times$

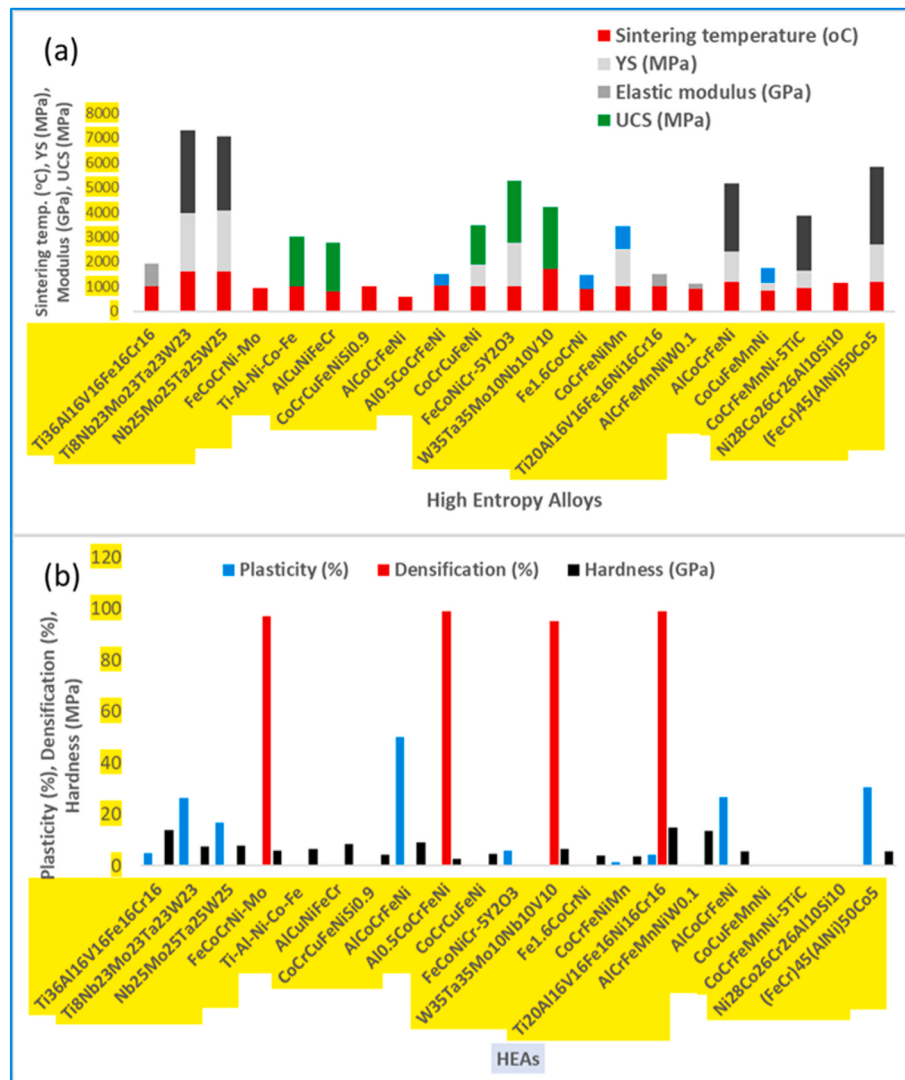


Fig. 5. Plots of the mechanical properties of some produced HEAs, (a) sintering temperature, yield stress, ultimate compressive stress and modulus of elasticity; (b) plasticity, densification and hardness of HEAs [24,33,45–61].

10^{-6} to $11.25 \times 10^{-6} \text{ K}^{-1}$, and drops monotonically with increase in Al concentration. Since Al induces the formation of BCC phases like in FeCoNiCrAl, FeCoNiAl_{0.2}Si_{0.2}, this equally implies that TEC drops when FCC structures like FeCoNi, FeCoNiCr, FeCoNiCrCu, FeCoNiCrPd HEAs, transforms to BCC structure [75]. Inoue et al. [76] characterized HEAs containing Al and compared their thermal diffusivity with pure Al. The result is as shown in Fig. 7. It can be observed from Fig. 6 that thermal diffusivity of Al, just like most other monolithic metals decrease as the temperature increases. This could be explained by scattering of the electrons and phonons as a result of increase in their vibrations occasioned by high temperature. However, the thermal diffusivity of the Al-containing HEAs increased, though sluggishly, with increase in the temperature. This could have been caused by phonon mean free path at higher temperature, due to thermal expansion of the lattice [77].

$$\text{Diffusivity, } \alpha = k / \rho C_p \Rightarrow k = \alpha \rho C_p \quad (\text{ii})$$

where α is the thermal conductivity, ρ is the density of the alloy and C_p is the specific heat capacity of the bulk mass. Using equation (ii) the thermal conductivities of the plotted HEAs can be calculated. From the equation (ii), it could be seen that diffusivity and conductivity are directly related. That implies that addition of Al in HEAs induces enhancement of thermal conductivity too.

Uporov et al. [72] characterized the thermal properties of ScTiZrHf

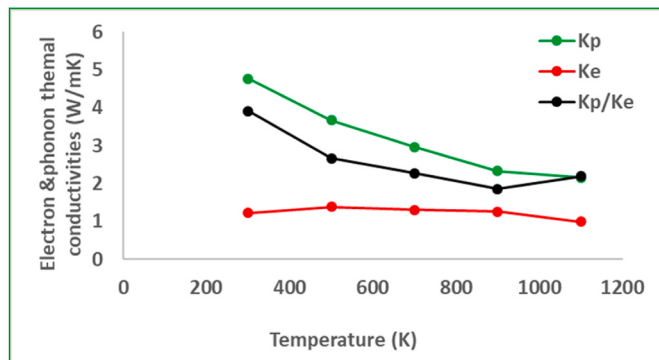
HEA. It was observed that metallic bonding dominated ScTiZrHf structural configuration, and that the thermal conductivity increased with increasing temperature. The arrangement of atoms in the crystals was so ordered that increase in the temperature did not distort the movement of electrons/phonons. It could equally be that there was improved phonon mean free path at higher temperature, due to thermal expansion of the lattice [77]. Meanwhile, the HEA possessed low thermal conductivity of 11.00 W/m. K at 700 K because of the hexagonal crystalline structure and defects in its crystal lattice. Dewangan et al. [78] studied the oxidation resistance of AlCuCrFeMn-W_x HEA prepared by MA + SPS with three weight percentages of W = 0.05, 0.1 and 0.5. The oxidation reaction was at 500 °C for 50 h, and the result showed that increase in the concentration of W increased the oxidation resistance of the alloy. The improvement was attributed to the increased steadiness and internal position of the WO₃ scale.

By and large, thermal conductivity of HEAs are generally lower than thermal conductivity of the individual metal elements that make up the alloy because of the following facts [79]: (i) irregular arrangement of atoms in the crystal structure does not give electrons, phonons or magnons free movement to transmit heat, (ii) non-uniform grains configuration in HEAs distort free flow of heat, (iii) multiply number of interfacial grain boundaries impede free flow of heat, (iv) multiple defects including dislocation, slip, vacancies obstruct free flow of heat in

Table 1

Comparative Characteristics of HEAs vis-a-vis Conventional Alloys.

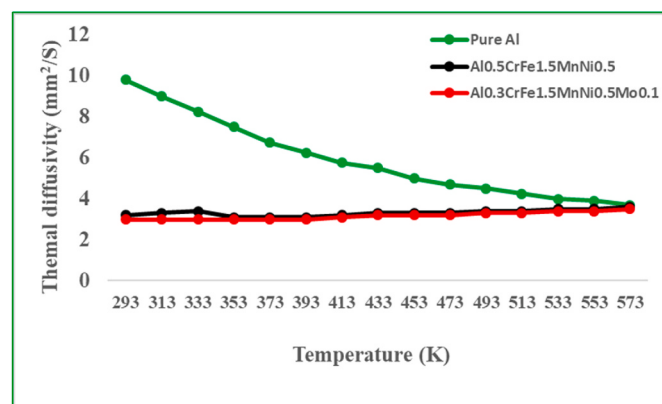
| High Entropy Alloys | Conventional Alloys | Ref |
|---|--|------|
| Most HEAs have complex microstructure that combines high hardness and ductility. | Most often, high hardness of conventional alloys is usually compromised by its ductility. | [62] |
| The equiatomic or near-equiatomic configuration of HEA gives it the property not to have principal alloying element which is the reason for high resistance to corrosion and oxidation. | The presence of primary alloying element in conventional alloys endanger its corrosion and oxidation resistance as galvanic potentials are easily set up in the configuration. | [63] |
| The high entropy effect of HEAs stimulates the generation of fine/nanocrystalline grains which enhances their mechanical strength. | Entropy of formation effect is low in conventional alloys, hence, strength from such effect is lacking. | [64] |
| The formation of solid solution and its strengthening in HEAs improve their thermal stability in a large range of high temperatures and compositions. | Solid solution strengthening is not universally obtained in conventional alloys. Hence, thermal stability as a result of that is absent. | [65] |
| The solid solution strengthening in HEAs equips it with multiple slip systems and this enhances its strength and ductility. | Most conventional alloys compromise mechanical strength, hardness for ductility. | [66] |
| Low chemical reactivity of HEAs decreases microstructural segregation and embrittlement. | Conventional alloys are affected by chemical segregation and embrittlement. | [67] |
| Sluggish diffusion effect in HEAs suppresses grain growth and recrystallization of microstructure. | There is no sluggish diffusion effect in conventional alloys, so, grain coarsening always accompanies its formation. | [68] |
| Cock tail effects in HEAs enable synergistic contribution of unlimited properties from multiple elements | Fewer elements are involved in the formation and the property may be limited | [69] |

**Fig. 6.** Variation of Electron and Phonon Thermal Conductivities of Al0.3CoCrFeNi with Temperature and their Ratio [73].

HEAs, severe lattice distortion. However, HEAs have high thermal stability because of the following reasons: (i) high entropy of mixing (configurational entropy) – high entropy of mixing translates to high thermal stability; (ii) huge number of atomic configuration leading to difficulty in phase transition; (iii) high melting point of the amalgamated elements making phase change difficult. Meanwhile, comparative analysis of HEAs and conventional alloys is presented in Table 2.

2.3. Microstructure of high entropy alloys

The microstructure of HEAs is usually different from the microstructure of the regular or conventional alloys. This is because of high level of arbitrariness or disturbances at their atomic level. This uncertainty is provoked by the large number of dissimilar elements coming together to form a HEA. However, microstructures of SPSed HEAs are

**Fig. 7.** Plot of thermal diffusivity of pure Al, Al0.5CrFe1.5MnNi0.5 and Al0.3CrFe1.5MnNi0.5Mo0.1 alloys.**Table 2**

Comparison of Thermal Properties of HEAs vis-à-vis Conventional Alloy.

| High Entropy Alloys (HEAs) | Conventional Alloys (CAs) | Ref |
|---|---|------|
| HEAs have disordered atomic configuration that leads to lower thermal expansion which increases its thermal stability. | The atomic configuration of conventional alloys is more ordered which leads to a higher thermal expansion and lower thermal stability. | [80] |
| The disordered microstructural configuration of HEAs leads to increased phonon scattering and lower thermal conductivity useful in heat shield and insulators | There is more ordered structural configuration in CAs leading to higher thermal conductivity and are not suitable in thermal shielding. | [81] |
| Large number of different elements in HEAs with different atomic radii leads to higher phonon scattering and subsequent lower diffusivity. | Fewer number of atoms make up conventional alloys and leads to fewer scattering of phonon and subsequent higher diffusivity. | [82] |
| A high number of dissimilar atomic sites in HEAs contributes to higher phonon scattering lowering thermal conductivity. | The atomic sites are similar in conventional alloys and heat transfer is more organized and accelerated. | [83] |
| The short-range order exhibited by HEAs decreases their lattice thermal conductivity, most often in most HEAs. | The long-range order in conventional alloys increases their thermal conductivity | [79] |
| The short-range order increases grain boundaries and reduces dislocation motion, leading to higher thermal stability. | The long range order supports dislocation motion and contributes to lower thermal stability in CAs | [79] |
| The large entropy of formation of HEAs results to larger activation energy of diffusion, which suppresses grain growth and increases thermal stability. | The activation energy of diffusion is lower in conventional alloys than in HEAs, so, thermal stability is usually lower. | [84] |
| HEAs have large vacancy densities and this decreases their thermal conductivity and improves their thermal resistance. | Conventional alloys have fewer vacancy densities, which leads to higher thermal conductivity and lower resistance. | [85] |
| The high-entropy point defects in HEAs increase photon scattering and reduce their thermal conductivity. | Low-entropy point defects in conventional alloys support higher thermal conductivity. | [86] |
| HEAs generate refined and nanocrystalline grains which reduce thermal transport, and lead to higher thermal stability. | Conventional alloys exhibit increased thermal transport with lower thermal stability. | [87] |

usually refined, having their grain sizes reduced to nanometers which usually improves their properties like strength [88], fracture toughness [89], thermal stability [55] and wear/corrosion resistance [59,90]. However, high degree of randomness accompanying consolidated HEA leads to the evolution of new phases in the microstructure. The formation of new phases influences the thermal, mechanical and tribological

characteristics of the consolidated alloy. Hence, it is through the manipulation of the new phases to be formed that materials with required characteristics for specific applications are produced. The new phases can be altered through selection of elements or manipulation of sintering parameters. Ujah et al. [45] produced $\text{Ti}_{36}\text{-Al}_{16}\text{-V}_{16}\text{-Fe}_{16}\text{-Cr}_{16}$ HEA using SPS. The authors observed that the alteration of sintering temperature controlled the formation of phases. When the sintering temperature was $1000\text{ }^{\circ}\text{C}$, BCC and FCC phases crystallized (Fig. 8a). But when it increased to $1100\text{ }^{\circ}\text{C}$, the two phases collapsed into only FCC (Fig. 8b and c). This led to the decrease in hardness and increase in ductility. As can be seen in Fig. 7a, the microstructure comprised Fe-rich FCC phase and Ti-rich BCC, while Fig. 8b is only Fe-rich FCC phase. Another microstructural characteristic of SPSed HEAs is formation of a brittle intermetallic phase known as sigma (σ -phases). This type of phase is formed when some typical elements (existing in some critical quantity) coagulate to form a compound with some unique crystal structure. HEAs which contain the following elements at certain quantities: aluminium, titanium, niobium, and molybdenum, are likely to form sigma phases. The evolution of sigma phases can be inhibited by altering the constitution of the alloy or by process parameter control. Most often, sigma phase is considered deleterious. Lu et al. [91] referred to it as a “harmful phase leading to serious embrittlement”. However, it may be beneficial to the alloy in some other times as it boosts the alloys’ wear

resistance, thermal stability and reduces porosity and dislocation [53, 92, 93].

Zhang et al. [94] produced $\text{Co}_{34.5}\text{Cr}_{30}\text{Ni}_{26.5}\text{Al}_{5.4}\text{W}_{3.6}$ HEA and characterized its properties. After the consolidation, it was found that the microstructure consisted of FCC matrix and sigma (σ) particles. Mechanical testing showed high ultimate tensile strength and ductility of the alloy which was attributed to the presence of FCC phase with a high strain hardening component (σ -particles) which induced uniform deformation and hindered crack propagation. It was discovered by another researcher that the introduction of V promoted the precipitation of sigma (σ) particles in CoCrCuFeNi HEA which was the principal factor that improved the compressive stress from 300 to 613 MPa (over 104 %) [95]. Transformation of phases usually accompanied SPS of HEAs. There is transformation from body-centered cubic (BCC) structure to face-centered cubic (FCC) structure and vice versa, in a process called solid-state phase transformation [96]. This phenomenon is influenced by the stacking fault energy (SFE) of the HEA [97]. Stacking fault energies of some FCC structured HEAs are shown in Fig. 9a. It will be recalled that SFE is the energy needed to arrange atoms in the crystal in a disordered form (Fig. 9b) which is a defect in the alloy’s configuration. HEAs with high SFE are more prone to transform to FCC, but those with low SFE usually remains in BCC or transform to BCC.

When the composition of the HEA includes Al, Cu or Ni [98], there is

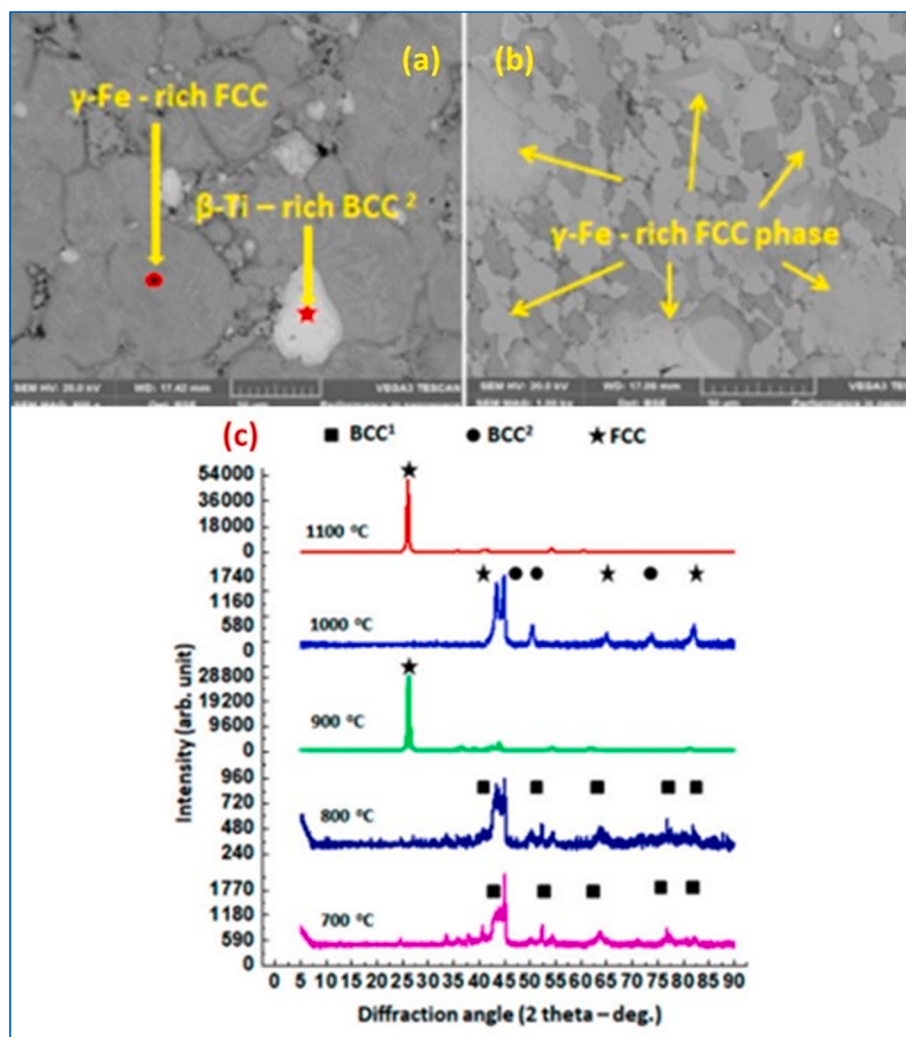


Fig. 8. Microstructure of $\text{Ti}_{36}\text{-Al}_{16}\text{-V}_{16}\text{-Fe}_{16}\text{-Cr}_{16}$ showing collapse of BCC and FCC into FCC (a) SEM of $\text{Ti}_{36}\text{-Al}_{16}\text{-V}_{16}\text{-Fe}_{16}\text{-Cr}_{16}$ sintered at $1000\text{ }^{\circ}\text{C}$ (b) SEM of $\text{Ti}_{36}\text{-Al}_{16}\text{-V}_{16}\text{-Fe}_{16}\text{-Cr}_{16}$ sintered at $1100\text{ }^{\circ}\text{C}$ (c) XRD showing peaks formed at various sintering temperatures [45].

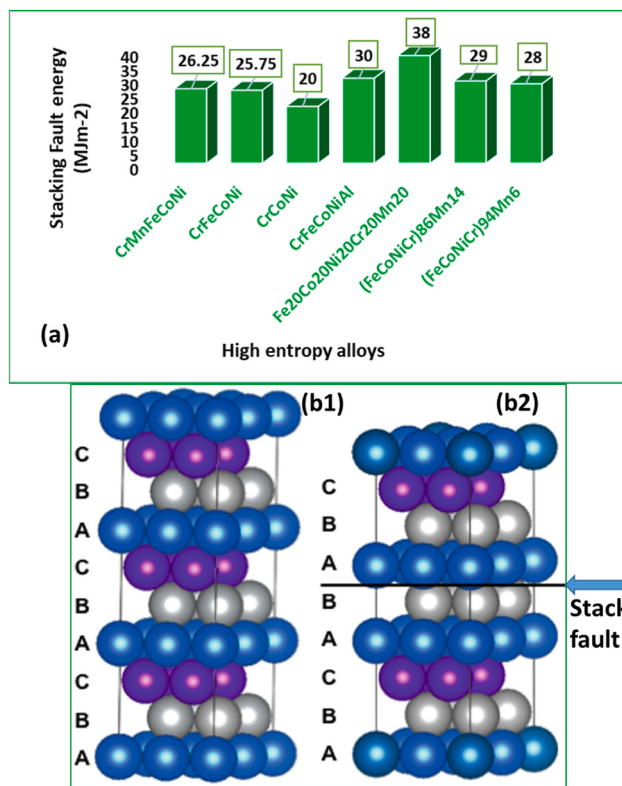


Fig. 9. Plots showing (a) stacking faults energy of some FCC HEAs, (b1) normal FCC structure (b2) stacking fault defect in FCC structure [98,99,102].

the tendency that it will possess high SFE. This tendency affects the mechanical strength like the yield and ductility of the HEA. By and large, FCC alloys usually have lower SFE [99] and exhibit higher ductility; while BCC alloys possess higher SFE with higher strength and tendency to embrittlement [100]. Thus, that is the major reason why FCC alloys have higher tendency to dislocation, higher slip system and more readily deformed plastically than BCC [101,102]. From Fig. 9a, CrCoNi alloy possessed lowest SFE while Fe₂₀Co₂₀Ni₂₀Cr₂₀ possessed highest SFE, so the dislocation density as well as ductility was higher in CrCoNi and lower in Fe₂₀Co₂₀Ni₂₀Cr₂₀. It will be confirmed from Fig. 9 that manipulation of the quantities of the constituent elements controls the phases and properties of HEA, as seen in Fe₂₀Co₂₀Ni₂₀Cr₂₀, (FeCoNiCr)₈₆Mn₁₄ and (FeCoNiCr)₉₄Mn₆ with the same elements at different compositions possessing different SFE.

Another characteristic feature of the microstructure of HEAs is the formation of intermetallic compound called Laves phase. The Laves phase (including TiFe₂, NbFe₂, and MgCu₂) precipitate, named after Fritz Laves who described it first in 1930s [103], is hard, brittle and prone to cracking. It consists of atoms arranged in an alternating layers in a rhombohedral unit cell as shown in Fig. 9a. Report has it that precipitation of Laves phase induces loss of ductility in the HEA. In a study to analyze the effect of Nb addition to CoCrCuFeNi HEA, Qin et al. [104] observed that when 16 at.% Nb was added to the HEA, the compressive yield strength increased from 338 MPa to 1322 MPa while the fracture strain reduced from 60.0 % to 8.1 %. The improvement in the yield and decrease in the ductility were stimulated by the precipitated Laves phase in the microstructure of the HEA.

More so, the presence of Laves phase in the microstructure diminishes thermal stability and corrosion resistance [105]. But, even though Laves phase reduces the ductility and thermal stability of HEAs, it improves their strength and hardness [106]. Such strong and hard materials are useful in defense and aeroplane applications. Its hard nature can be a protective layer to prevent corrosion and can be applied in marine industries. The formation of Laves phase can be controlled or

altered by careful selection of elements to be used, optimizing the sintering parameters [107] and addition of cushioning elements like C, Fe, N₂, and B [108,109].

One more important phase that precipitates in HEA is the Topologically close-packed (TCP) phase. It has close-packed arrangement of atoms in its crystal structure as shown in Fig. 10b. Due to the arrangements of the atoms in TCP, it is more thermodynamically stable than other precipitates. It has high hardness and brittleness but low ductility, poor creep and high nucleation sites for fracture [110–112]. However, it has high thermal stability, high oxidation resistance, and high strength. These properties make the phase good for applications in high temperature industrial components. One of the ways to control the precipitation of TCP is by reducing the percentage of Al, Ta and Ti in the alloy [112].

Meanwhile, evolution of phases can be manipulated by the addition of specific elements in the HEA matrices. This was evidenced in the study conducted by Oh et al. [115] where AlCoCrFeNi HEA was tailored to generate various phases by the addition of Mg, Ti, Mn, Cu, and Zn, in separate consolidation with SPS at 1000 °C preceded by MA for 30 h. Results show that addition of Mg evoked the formation of ordered BCC/B2 phase, and addition of Ti (AlCoCrFeNi-Ti) led to evolution of the same BCC/B2 phase. But in AlCoCrFeNi-Cu and AlCoCrFeNi-Zn HEAs, there were evolution of both FCC and minute BCC phases. Then in AlCoCrFeNi and AlCoCrFeNi-Mn, the authors observed formation of sigma (σ) phase in a BCC matrix with minor FCC phase. Amongst all the tested HEAs, AlCoCrFeNi-Mn displayed the maximum compressive strength because of the formed σ -phase and ordered BCC/B2 phase. In another study, Sharma et al. [116] investigated the effect of adding Cr, Mn, Zn, Sn elements on AlCuSiFe-x HEA using MA for 45 h and SPS at 650 °C. AlCuSiFe-Zn and AlCuSiFe-Sn showed the formation of BCC + FCC after mechanical alloying, while BCC single phase was observed when Mn and Cr were added. But after SPS, AlCuSiFe-Sn HEA generated FCC phase and Cu_xSn_y precipitate, and there was evolution of FCC + BCC phases in AlCuSiFe-Zn. Also, AlCuSiFe-Cr and AlCuSiFe-Mn formed BCC + FCC with σ - and μ -phases. When the thermodynamic parameters of the AlCuSiFe-X HEAs were computed, it was realized that incorporation of Sn and Zn stimulated the evolution of FCC phase, while that of Cr and Mn evoked the formation of BCC along with hard μ and σ phases, and these hard precipitates improved their mechanical strengths [117]. Oh et al. [118], more so, investigated the effect of Cu, Mn, and Ti elements on the microstructure and mechanical properties of AlCoCrFeNi-X HEAs prepared by MA for 30 h at 300 rpm, followed by SPS at 1000 °C. There was evolution of sigma (σ), FCC, BCC-phases with ordered BCC (B2) precipitates in AlCoCrFeNi and AlCoCrFeNi-Mn HEAs, while AlCoCrFeNi-Cu generated FCC and BCC with ordered BCC (B2) precipitate; there was formation of only BCC/B2 phase in AlCoCrFeNi-Ti HEA. The evolution of BCC/B2 and hard σ -particles enabled AlCoCrFeNi-Mn and AlCoCrFeNi-Ti possess superior strength over other HEA samples tested. Chae et al. [119] studied the effect of

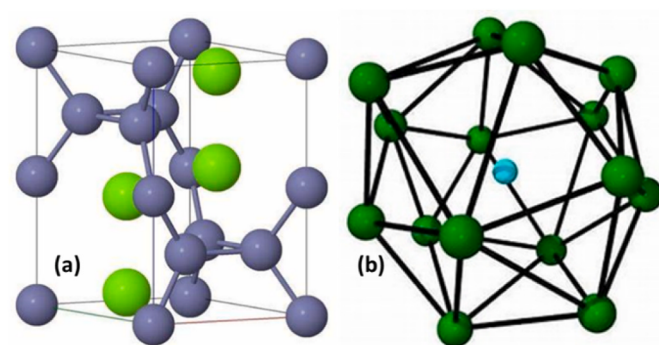


Fig. 10. Crystal structures of phases prevalent in HEAs (a) laves phase (b) topological close-packed phase [113,114].

addition of light metals, (Mg and Si), and heavy metal, Zn, on the microstructural evolution of AlCuFeMnTi-X HEA using MA for 45 h, followed by SPS at 700 °C. After MA, BCC1 and BCC2 were formed on all the alloy. Volume fraction of BCC2 was largest in AlCuFeMnTi-Zn when compared with other samples. AlCuFeMnTi-Si HEA had large fraction of BCC2 but lower than that of AlCuFeMnTi-Zn. After SPS, the highest hardness was recorded in AlCuFeMnTi-Mg as a result of the evolved Cu₂Mg particles in a BCC2/BCC1 matrix.

3. Applications of high entropy alloys

The uniqueness of HEAs is the reason behind its usage in a plethora of applications. They have versatile applications because it has unique properties quite more superior than conventional alloys. Their excellent mechanical, microstructural, thermal and physical properties have made them enviable materials for applications in aerospace, automotive, medical, pharmaceutical, energy, and structural industries.

A) Aerospace industry: Aerospace components were traditionally built with superalloys and single crystal alloys. However, the narrative is changing since the discovery of HEAs. Due to their high thermal stability and high strength at elevated temperatures, HEAs are being used to replace those conventional alloys employed in jet engine components like the turbine blades, compressors, and combustor. Fig. 11 shows a jet engine with its components where HEAs are being used to replace traditional alloys. As can be seen in Fig. 11, the rotor was hitherto built with ferritic steel. But it has been disclosed that GE Aviation has developed NbMoTaW HEA which possess better properties than ferritic steel [120]. Such properties include: withstanding temperature over 800 °C, very high strength and high corrosion resistance at elevated temperatures with sound creep resistance. Other HEAs represented in Fig. 11 of the jet engine have higher resistance to wear, corrosion, oxidation, fatigue, creep than the conventional superalloys/single crystal alloys.

Materials that need to be removed and replaced with HEAs in aerospace body parts abound. One of them is the nickel-based superalloys that are presently being used in the elevated temperature components of jet engines. Ni-based alloys are very costly and very difficult to process. Therefore, substituting them with HEAs would definitely make the jet engine more affordable, processable and efficient. More so, Ti-based alloys are recommended to be replaced with HEAs in

development of aircraft parts. This is because HEAs are more processable and cost effective.

- B) Automotive industry: The high strength without compromising ductility of HEAs makes it a novel material for the production of robust automotive components like engine valves, gears, brake calipers, shafts, connecting rods, engine pistons and ball joints. Other properties displayed by HEAs requisite for their application in automotive industries include resistance to fatigue load, resistance to corrosion, wear and impact loads. AlCoCrFeNi HEA is light, has high yield strength of 1263 MPa at 773 K, high ultimate compressive strength (UCS) of 1702 MPa and plasticity of 19.9 % up to the temperature of 773 K. This shows that it is suitable for use in structural and high temperature applications like gears, engine pistons and valves [122].
- C) Nautical and maritime devices: High strength-to-weight ratio and excellent corrosion resistance make HEAs novel material for use in maritime industry. Submarine machines come in contact with salt water which corrodes easily. So, components used in producing such devices should have top notch corrosion resistance, as well as low density. Nickel-based HEA called MAR-M247 (NiCr₁₆Co₁₁Mo₄) is one of the best alloys in building maritime ships and boats.
- D) Biomedical applications: Popescu et al. [123] developed TiZrNbTaFe HEA and characterized its properties for biomedical implants. This HEA was compared with the conventional implant, Ti6Al4V alloy. It was reported that corrosion affects Ti64 heavily because of the presence of α and β phases in the microstructure which initiate galvanic corrosion at their interfaces. But the novel HEA exhibited only β phase which is more resistant to corrosion. More so, the presence of Ta increased the resistance of the HEA to corrosion because it is very resistant to Cl⁻ by forming Ta₂O₅ protective film. It was therefore concluded that TiZrNbTaFe HEA is more biocompatible than Ti6Al4V for biomedical applications. Two major ways by which HEAs are employed in medical sector are in orthopedic implants (comprising hip and knee), and in dental implants. HEAs employed for hip and knee replacements usually possess high strength, low elasticity and high biocompatibility; which are properties they share with natural human bones. CoCrFeMnNi HEA has been successfully applied in the replacement of hip and knee and has exhibited superior characteristics in clinical trials [124]. For dental replacement, CoCrFe-NiMnMo HEA has shown exceptional corrosion resistance, high

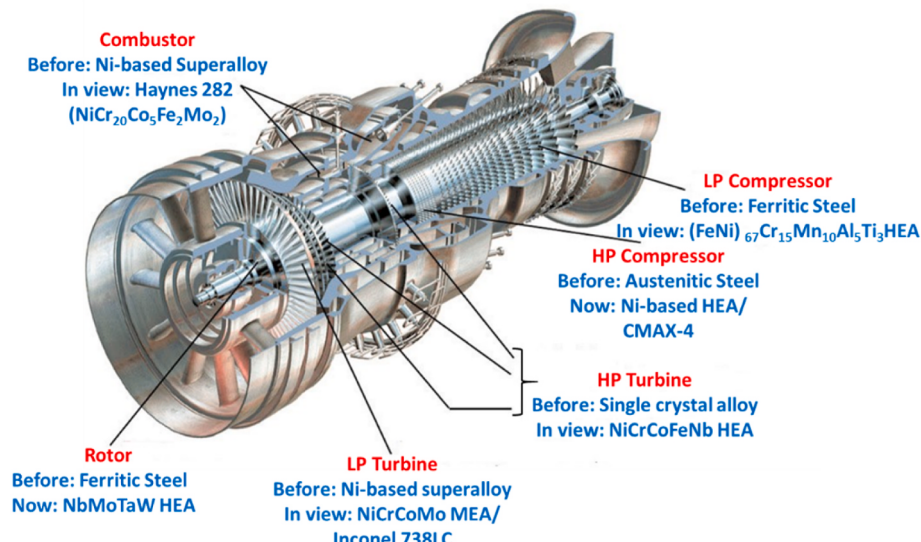


Fig. 11. Components of jet engine [121].

tribology characteristics, good biocompatibility and high strength. It equally commands good formability and shaping. Most conventional synthetic drugs which need to be substituted by HEAs include statins, antibiotics, and anti-cancer drugs. Statins, like atorvastatin and simvastatin are drugs for the treatment of high cholesterol [125]. But these drugs have some side effects like pains in the muscles, damaging of liver, and dementia. Conventional anti-cancer drugs like doxorubicin and cyclophosphamide are used to treat various types of cancer [126]. But they have side effects like hair loss, nausea, vomiting, diarrhea, and loss of appetite. Interestingly, anti-cancer HEA drug called Ruthenium (II) tris(bipyridine) chloride ($C_{36}H_{36}Cl_2N_6O_6Ru$) has shown high cytotoxic proficiency against cancer cell lines, like breast cancer, and prostate cancer, with little or no known side effects [127].

- E) HEAs for electrocatalysis: Fuel cells generate electricity by the electrochemical reaction producing only water as the by-product. In H_2 fuel cell, H_2 is broken down into electron and proton. The electron is whisked away as electricity while the proton collides with molecules of O_2 to form water by-product. However, when a specialized HEA like IrPdPtRhRu is introduced into fuel cell, it aids as a catalyst for oxygen reduction reaction (ORR) which catalyzes/reduces the oxygen in the cell into water and electron (electricity), instead of being burned to produce electricity. Reduction takes place at very lower temperature than burning, hence, ORR is very efficient in electricity generation. According to Batchelor et al. [128], HEAs can offer a platform with a very gigantic number of special binding sites which will culminate to a near-continuous supply of related adsorption energies, like in the case of ORR. CrMnFeCoNi HEA is being researched on for the use in ORR for fuel cells by Loffler and his team [129]. Electrocatalytic HEAs are being incorporated into fuel cells like proton exchange membrane fuel cells (PEMFCs) and solid oxide fuel cells (SOFCs) to improve their versatility, efficiency, longevity and sustainability as their operating temperatures and pressures are drastically reduced.
- F) Hydrogen energy storage: Conventionally, metal hydrides like MgH_2 and $NaAlH_4$ are useful in storing hydrogen energy. Ideally, they have maximum hydrogen-to-metal (H/M) ratio of 2. Meanwhile, since the advent of HEAs, research has shown that they can have H/M ratio of 2.5 or more. Such HEAs as $TiVZrNbHf$ has the capacity to store higher quantity of H_2 than its constituent elements. This property is attributed to the large lattice strain in the alloy which creates an enabling environment to absorb hydrogen in both tetrahedral and octahedral interstitial sites [130].
- G) Military facilities and equipment: Military is another sector that finds the application of HEAs very crucial especially in military vehicles, protective shields, and armories. The high performance of HEAs in military sector is attributed to their high strength and hardness, resistance to corrosion and wear, high impact strength and high fatigue resistance [131]. An alloy comprising NiCoFeVMo referred as AerMet 100 is a HEA employed in the production of ammunition casing because of its excellent performance in wear and impact resistance. Tang and Li [132] employed molecular dynamics simulations to study the ballistic performance of CrMnFeCoNi and CrFeCoNi HEAs in order to understand their resistance propensity kinetics. They observed that the alloys' ballistic resistances are anchored on the active dislocations produced at higher strain rates. Stouter atomic bonding and larger dislocation densities enable CrFeCoNi HEA to be strain-hardened more easily resulting in increased toughness to withstand high-speed deformation; while less-stout atomic bonding and lesser dislocation densities make CrMnFeCoNi more vulnerable to failure under ballistic attack. Hence, the presence of Mn reduces the impact energy of ballistic-resistant HEAs.

H) Water purification: HEAs have high adsorption property as a result of their high surface area which provides large area for adsorption of contaminants. More so, the high degree of disorder in HEAs enables them to possess large binding sites for the water contaminants. The high disorder will not give the contaminants a safe haven to pile up and cause fouling in the water channel [133]; coupled with their refined microstructure. It was reported that CoCrFeMnNi HEA is a good anti-fouling agent in water purification. Furthermore, HEAs have refined microstructure devoid of pores which does not give binding sites for water contaminants. Contaminants bonds better on coarse and porous surface and wreck their havoc. Worthy of note equally is that HEAs have high corrosion resistance and superhydrophobicity [134]. So, microorganisms with high affinity to inhabiting on corroded surfaces are dearth in surfaces cladded with HEAs because of lack of corrosion ions or radicals.

- I) Microjoining: HEAs can perform more efficiently than conventional alloys in joining small components with the application of pressure and heat [135]. This is because HEAs possess higher strength, higher thermal properties with low weight. HEAs joining is useful in the production of MEMS (Micro-Electro-Mechanical Systems) devices like sensors and actuators together with repairing their small parts [136]. The high strength of HEAs is required to withstand high stresses domiciled in a joint. Low weight is requisite in today's need in miniaturization innovations of components and products, hence, the need for use of HEAs. Replacing conventional alloys with HEAs for high thermal applications is imperative because refractory HEAs can withstand high temperatures without losing strength coupled with high creep resistance. FeCrAl-XY HEA (XY = Si, C, N, B), for instance can be applied for elevated temperature joining as they can withstand temperature of up to 1450 °C with appreciable oxidation and corrosion resistance [137].

4. Challenges of SPS of HEAs and future work

4.1. Challenges

The spark plasma sintering of high entropy alloys faces many challenges as HEAs are relatively new subject area that has not transcended two decades.

One of the general challenges in the development of HEAs is choosing the right and adequate mixture of elements which will give the desired characteristics. This is difficult because it is just a minute combination of these elements that have been empirically tested and published. Hence, most other combinations are yet to be experimented and no information is available about them in the open literature. So, present experiments in the development of HEAs is based on trial and error.

It is very unfortunate that only few information is available on the theoretical behaviours of high entropy alloys, let alone those prepared with SPS. So, it is still a herculean task to predict their properties at various conditions and for various applications bearing in mind that their multiple compositions are actually a complexity. Hence, design and development of HEAs for specific applications are still a very difficult task.

The exorbitant cost of raw materials and SPS machinery is another challenge in the development and commercialization of HEAs. Most elements employed in the development of HEAs are rare metals or rare earth metals which are very expensive. In the world market, for instance, 28.35 g of rhodium is valued at \$25,000.00; very costly [138]. Other metals like Au, Sc, Pt, Nd, Pd, Ir are very expensive and that makes development of HEAs not yet cost effective and affordable. More so, SPS technique is still not commercially viable as its scalability has not been fully actualized [139].

Furthermore, manipulation and control of the microstructure of HEAs may not be as easy as it is with conventional alloys because the

degree of disorder during their formation is very high. Ordinarily, SPS suppresses grain growth and pore formation in conventional composites and alloys [140]. However, the case of HEAs is different because elements with different atomic configurations and radii, together with varying melting temperatures are locked up together to form a single entity. Hence, some of the elements may attain melting temperature while others are yet to attain theirs during sintering, thereby generating heterogeneous microstructure with possible grain coarsening.

The degree of disorder in HEAs, their cumulative large atomic configuration and inhomogeneous microstructure coupled with the mode of heating exhibited by SPS induce thermal gradient and consequent thermal stress in SPSed HEAs. Thermally stressed alloys have every tendency to fail from residual stresses and cracks. It should be recalled that cracks are the nucleation sites for failure.

4.2. Future works

Further research on the correlation between the microstructure and physical, mechanical, thermal, and other properties of HEAs is urgently imperative. This is because the theoretical data linking the properties and microstructure is scarce in the literature. Mores so, the relationship between the sintering parameters and phase evolution and microstructure are not sufficiently available in the literature. Proliferation of such information would skyrocket the advancement of HEAs for technological advancement.

Information correlating the composition of HEAs and processing parameters is scarce in the literature. Dearth in the open literature also is relationship between the particle size, melting temperature, density and the microstructure of the accruing HEAs. It will be very crucial and a resounding breakthrough if research on how some of the itemized properties influence the microstructure or properties of the HEAs is urgently handled.

More works on modeling and simulation of HEAs are not only imperative but timely to be revolutionized. This model would help to predict the properties that would evolve under certain conditions, and optimize process parameter. Such models will eliminate trial and error method of research which is costlier and more time consuming despite that it has very low success rate. This maxim is supported by Dewangan et al. [141] who opined that despite numerous laboratory trials, dearth of empirical data are still an issue of major concern for research and innovation.

It was stated that SPS generates bulk materials infested with thermal stress originating from non-homogenous heating of the inner and outer surfaces of the bulk samples. To this end, further research is encouraged on how to reduce this thermal gradient through the use of computer-aided manufacturing or infrared thermography.

Further research is encouraged on improving the cost effectiveness of SPS; there is the need for more work on the economic feasibility of SPS, including the development of more cost-effective equipment and processes.

5. Conclusion and recommendation

Review of published articles in the open literature of HEAs has been concluded and the following salient points were obtained.

- A) HEAs have prospective applications in aerospace, medical, pharmaceutical, electrical and engineering applications because of their superior properties which are more robust than that of conventional and super alloys.
- B) Mechanical properties of HEAs are dependent on the phases exhibited by the alloy. BCC structured HEAs have high strength and hardness, while FCC structured HEAs possess high ductility and strength.
- C) Presence of Al in HEAs induces the formation B2 (ordered body-centered-cubic) structure which is thermodynamically stable and

induces increment in strength and ductility at the same time in HEAs. Presence of Al equally induces increment of thermal conductivity and diffusivity in HEAs.

- D) Desirable microstructural phases can be produced through the manipulation of sintering parameters or selection of elements and their concentration. Addition of Al, Ti, Nb, V and Mo induce the evolution of sigma phase which increases strength, wear resistance and thermal stability; and reduces porosity and dislocation in HEAs. FCC structured alloys have lower stacking fault energy and exhibit higher ductility; while BCC structured alloys possess higher SFE with higher strength and tendency to embrittlement. Al, Cu and Ni induce high SFE.

Recommendation for Future Work.

- A) Information on SPS of HEAs is still limited in the literature. Scalability of SPS products is also another big challenge. So, it is recommended that more experimental works on SPS of HEAs should be carried out, and publication of more journal articles and review articles on this topic is critically imperative in order to bring HEAs into the pedestal it ought to be.

Declaration of competing interest

The authors declare that they have no known competing financial interests or personal relationships that could have appeared to influence the work reported in this paper.

Data availability

Data will be made available on request.

References

- [1] B. Stojanovic, M. Bukvic, I. Epler, Application of aluminum and aluminum alloys in engineering, Applied Engineering Letters, Journal of Engineering and Applied Sciences 3 (2) (2018) 52–62.
- [2] R. Qin, et al., Effect of sintering temperature on microstructure characteristics and damping capacity of multilayer 316L stainless steel hollow spheres/A356 alloy composites reinforced by NiTi alloy sheets, Mater. Sci. Eng., A 860 (2022) 144321.
- [3] S. Liu, et al., Microstructure and properties of ceramic particle reinforced FeCoNiCrMnTi high entropy alloy laser cladding coating, Intermetallics 140 (2022) 107402.
- [4] A.K. Gupta, R. Velmurugan, M. Joshi, Comparative study of damping in pristine, steel, and shape memory alloy hybrid glass fiber reinforced plastic composite beams of equivalent stiffness, Defence Sci. J. 68 (1) (2018) 91.
- [5] C.M. Rost, et al., Entropy-stabilized oxides, Nat. Commun. 6 (1) (2015) 8485.
- [6] E. Strumza, et al., A comprehensive study of phase transitions in Al0.5CoCrFeNi high-entropy alloy at intermediate temperatures ($400 \leq T \leq 900^\circ\text{C}$), J. Alloys Compd. 898 (2022) 162955.
- [7] B. Cantor, et al., Microstructural development in equiatomic multicomponent alloys, Mater. Sci. Eng., A 375 (2004) 213–218.
- [8] J.W. Yeh, et al., Nanostructured high-entropy alloys with multiple principal elements: novel alloy design concepts and outcomes, Adv. Eng. Mater. 6 (5) (2004) 299–303.
- [9] J.-W. Yeh, Overview of high-entropy alloys, High-entropy alloys: fundamentals and applications (2016) 1–19.
- [10] C.O. Ujah, et al., Investigating the nanomechanical and thermal characteristics of Ti20-Al120-V20-Fe20-Ni20 HEA developed via SPS for high energy applications, Metallurgical Research & Technology 119 (6) (2022) 616.
- [11] M. Suárez, et al., Challenges and opportunities for spark plasma sintering: a key technology for a new generation of materials, Sintering applications 13 (2013) 319–342.
- [12] N. Weston, et al., Spark plasma sintering of commercial and development titanium alloy powders, J. Mater. Sci. 50 (2015) 4860–4878.
- [13] C. Ujah, et al., Optimisation of spark plasma sintering parameters of Al-CNTs-Nb nano-composite using Taguchi Design of Experiment, Int. J. Adv. Des. Manuf. Technol. 100 (2019) 1563–1573.
- [14] Z.-Y. Hu, et al., A review of multi-physical fields induced phenomena and effects in spark plasma sintering: fundamentals and applications, Mater. Des. 191 (2020) 108662.
- [15] S. Ma, et al., Effects of temperature on microstructure and mechanical properties of IN718 reinforced by reduced graphene oxide through spark plasma sintering, J. Alloys Compd. 767 (2018) 675–681.

- [16] J. Choi, et al., Fabrication of sintered tungsten by spark plasma sintering and investigation of thermal stability, *Int. J. Refract. Metals Hard Mater.* 69 (2017) 164–169.
- [17] Y. Long, et al., High entropy alloy borides prepared by powder metallurgy process and the enhanced fracture toughness by addition of yttrium, *Mater. Chem. Phys.* 257 (2021) 123715.
- [18] C. Ujah, et al., Enhanced mechanical, electrical and corrosion characteristics of Al-CNTs-Nb composite processed via spark plasma sintering for conductor core, *J. Compos. Mater.* 53 (26–27) (2019) 3775–3786.
- [19] I. Moravcik, et al., Microstructure and mechanical properties of Ni1, 5Co1, 5CrFeTi0, 5 high entropy alloy fabricated by mechanical alloying and spark plasma sintering, *Mater. Des.* 119 (2017) 141–150.
- [20] H. Zhang, et al., Ultrahigh strength induced by multiple heterostructures in a FeMnCoCrN high-entropy alloy fabricated by powder metallurgy technique, *Mater. Sci. Eng., A* 846 (2022) 143304.
- [21] B.C. Ocak, G. Goller, Investigation the effect of FeNiCrMo HEA addition on properties of B4C ceramic prepared by spark plasma sintering, *J. Eur. Ceram. Soc.* 41 (13) (2021) 6290–6301.
- [22] B. Kang, et al., Fabrication, microstructure and mechanical property of a novel Nb-rich refractory high-entropy alloy strengthened by in-situ formation of dispersoids, *Int. J. Refract. Metals Hard Mater.* 81 (2019) 15–20.
- [23] O.N. Senkov, et al., Mechanical properties of Nb25Mo25Ta25W25 and V20Nb20Mo20Ta20W20 refractory high entropy alloys, *Intermetallics* 19 (5) (2011) 698–706.
- [24] J. Pan, et al., Microstructure and mechanical properties of Nb25Mo25Ta25W25 and Ti8Nb23Mo23Ta23W23 high entropy alloys prepared by mechanical alloying and spark plasma sintering, *Mater. Sci. Eng., A* 738 (2018) 362–366.
- [25] Y. Sun, et al., Phases, microstructures and mechanical properties of CoCrNiCuZn high-entropy alloy prepared by mechanical alloying and spark plasma sintering, *Entropy* 21 (2) (2019) 122.
- [26] W. Pan, et al., Microstructure and mechanical properties of AlCoCrFeNi2, 1 eutectic high-entropy alloy synthesized by spark plasma sintering of gas-atomized powder, *Intermetallics* 144 (2022) 107523.
- [27] A. Kumar, A.K. Swarnkar, M. Chopkar, Phase evolution and mechanical properties of AlCoCrFeNiSi x high-entropy alloys synthesized by mechanical alloying and spark plasma sintering, *J. Mater. Eng. Perform.* 27 (2018) 3304–3314.
- [28] S. Yadav, et al., Wear and mechanical properties of novel (CuCrFeTiZn) 100-xPbx high entropy alloy composite via mechanical alloying and spark plasma sintering, *Wear* 410 (2018) 93–109.
- [29] A. Bahrami, A. Mohammadnejad, M. Sajadi, Microstructure and mechanical properties of spark plasma sintered AlCoFeMnNi high entropy alloy (HEA)-carbon nanotube (CNT) nanocomposite, *J. Alloys Compd.* 862 (2021) 158577.
- [30] A.I. Yurkova, et al., Structure formation and mechanical properties of the high-entropy AlCuNiFeCr alloy prepared by mechanical alloying and spark plasma sintering, *J. Alloys Compd.* 786 (2019) 139–148.
- [31] S.-P. Wang, J. Xu, TiZrNbTaMo high-entropy alloy designed for orthopedic implants: as-cast microstructure and mechanical properties, *Mater. Sci. Eng. C* 73 (2017) 80–89.
- [32] C. Zhu, et al., Microstructure and mechanical properties of the TiZrNbMoTa refractory high-entropy alloy produced by mechanical alloying and spark plasma sintering, *Int. J. Refract. Metals Hard Mater.* 93 (2020) 105357.
- [33] Y. Peng, et al., Microstructures and mechanical properties of FeCoCrNi-Mo High entropy alloys prepared by spark plasma sintering and vacuum hot-pressed sintering, *Mater. Today Commun.* 24 (2020) 101009.
- [34] C.O. Ujah, D.V.V. Kallon, V.S. Aigbodion, Tribological properties of CNTs-reinforced nano composite materials, *Lubricants* 11 (3) (2023) 95.
- [35] B. Wang, et al., Mechanical properties and microstructure of the CoCrFeMnNi high entropy alloy under high strain rate compression, *J. Mater. Eng. Perform.* 25 (2016) 2985–2992.
- [36] S. Mohanty, et al., Powder metallurgical processing of equiatomic AlCoCrFeNi high entropy alloy: microstructure and mechanical properties, *Mater. Sci. Eng., A* 679 (2017) 299–313.
- [37] H. Lee, A. Sharma, B. Ahn, Exploring strengthening mechanism of FeCoNiAl high-entropy alloy by non-metallic silicon addition produced via powder metallurgy, *J. Alloys Compd.* 947 (2023) 169545.
- [38] S.K. Dewangan, et al., Surface Morphology Transformation and Densification Behaviour of Conventionally Sintered AlFeCoNiSi High Entropy Alloys, *Powder Metallurgy*, 2023, pp. 1–12.
- [39] H. Lee, et al., Correlation between the Nanomechanical Characteristic and the Phase Transformation of BCC-Based High Entropy Alloys Produced via Powder Metallurgy, *Powder Metallurgy*, 2023, pp. 1–10.
- [40] C. Nagarjuna, et al., Microstructure, mechanical and tribological properties of oxide dispersion strengthened CoCrFeMnNi high-entropy alloys fabricated by powder metallurgy, *J. Mater. Res. Technol.* 22 (2023) 1708–1722.
- [41] A. Sharma, M.C. Oh, B. Ahn, Microstructural evolution and mechanical properties of non-Cantor AlCuSiZnFe lightweight high entropy alloy processed by advanced powder metallurgy, *Mater. Sci. Eng., A* 797 (2020) 140066.
- [42] S.K. Dewangan, et al., Prediction of nanoindentation creep behavior of tungsten-containing high entropy alloys using artificial neural network trained with Levenberg–Marquardt algorithm, *J. Alloys Compd.* 958 (2023) 170359.
- [43] C. Nagarjuna, et al., Application of artificial neural network to predict the crystallite size and lattice strain of CoCrFeMnNi high entropy alloy prepared by powder metallurgy, *Met. Mater. Int.* 29 (7) (2023) 1968–1975.
- [44] C. Ujah, et al., Analysis of the microstructure and tribology of Ti36-Al16-V16-Fe16-Cr16 HEA developed with SPS for engineering applications, *JOM* 74 (11) (2022) 4239–4249.
- [45] C.O. Ujah, et al., Mechanical and thermal behaviors of Ti36-Al16-V16-Fe16-Cr16 high entropy alloys fabricated by spark plasma sintering: an advanced material for high temperature/strength applications, *J. Compos. Mater.* 56 (26) (2022) 3913–3923.
- [46] R.A. Sekhar, et al., Microstructure and mechanical properties of Ti-Al-Ni-Co-Fe based high entropy alloys prepared by powder metallurgy route, *J. Alloys Compd.* 787 (2019) 123–132.
- [47] A. Kumar, et al., Effects of processing route on phase evolution and mechanical properties of CoCrCuFeNiSix high entropy alloys, *J. Alloys Compd.* 748 (2018) 889–897.
- [48] Y. Liu, et al., Formation of transition layer and its effect on mechanical properties of AlCoCrFeNi high-entropy alloy/Al composites, *J. Alloys Compd.* 780 (2019) 558–564.
- [49] K. Xiong, et al., Cooling-rate effect on microstructure and mechanical properties of Al0. 5CoCrFeNi high-entropy alloy, *Metals* 12 (8) (2022) 1254.
- [50] K.R. Rao, S.K. Sinha, Effect of sintering temperature on microstructural and mechanical properties of SPS processed CoCrCuFeNi based ODS high entropy alloy, *Mater. Chem. Phys.* 256 (2020) 123709.
- [51] B. Jia, et al., Microstructure and mechanical properties of FeCoNiCr high-entropy alloy strengthened by nano-Y 2 O 3 dispersion, *Sci. China Technol. Sci.* 61 (2018) 179–183.
- [52] X. Hu, et al., A high-density non-equiautomic WTaMoNbV high-entropy alloy: alloying behavior, microstructure and mechanical properties, *J. Alloys Compd.* 894 (2022) 162505.
- [53] P. Moazzeni, M.R. Toroghinejad, P. Cavaliere, Effect of Iron content on the microstructure evolution, mechanical properties and wear resistance of FeExCoCrNi high-entropy alloy system produced via MA-SPS, *J. Alloys Compd.* 870 (2021) 159410.
- [54] F. Průša, et al., Properties of a high-strength ultrafine-grained CoCrFeNiMn high-entropy alloy prepared by short-term mechanical alloying and spark plasma sintering, *Mater. Sci. Eng., A* 734 (2018) 341–352.
- [55] C. Ujah, et al., Mechanical and oxidation characteristics of Ti20-Al16-V16-Fe16-Ni16-Cr16 high-entropy alloy developed via spark plasma sintering for high-temperature/strength applications, *J. Mater. Eng. Perform.* 32 (1) (2023) 18–28.
- [56] S.K. Dewangan, et al., Microstructure and mechanical properties of nanocrystalline AlCrFeMnNiWx ($x = 0, 0.05, 0.1, 0.5$) high-entropy alloys prepared by powder metallurgy route, *J. Mater. Eng. Perform.* 30 (6) (2021) 4421–4431.
- [57] S. Xie, et al., Effect of heating rate on microstructure and mechanical properties of AlCoCrFeNi high entropy alloy produced by spark plasma sintering, *Mater. Char.* 154 (2019) 169–180.
- [58] M. Karimi, et al., Fabrication of a novel magnetic high entropy alloy with desirable mechanical properties by mechanical alloying and spark plasma sintering, *J. Manuf. Process.* 84 (2022) 859–870.
- [59] D. Yim, et al., Fabrication and mechanical properties of TiC reinforced CoCrFeMnNi high-entropy alloy composite by water atomization and spark plasma sintering, *J. Alloys Compd.* 781 (2019) 389–396.
- [60] A. Shahbazkhan, H. Sabet, M. Abbasi, Microstructural and mechanical properties of NiCoCrAlSi high entropy alloy fabricated by mechanical alloying and spark plasma sintering, *J. Alloys Compd.* 896 (2022) 163041.
- [61] Y. Xiao, X. Peng, T. Fu, A novel high-entropy alloy with multi-scale precipitates and excellent mechanical properties fabricated by spark plasma sintering, *Adv. Powder Technol.* 33 (3) (2022) 103520.
- [62] L. Chen, et al., Heavy carbon alloyed FCC-structured high entropy alloy with excellent combination of strength and ductility, *Mater. Sci. Eng., A* 716 (2018) 150–156.
- [63] T. Li, et al., Localized corrosion behavior of a single-phase non-equimolar high entropy alloy, *Electrochim. Acta* 306 (2019) 71–84.
- [64] M.S. Rizi, et al., Hierarchically activated deformation mechanisms to form ultrafine grain microstructure in carbon containing FeMnCoCr twinning induced plasticity high entropy alloy, *Mater. Sci. Eng., A* 824 (2021) 141803.
- [65] F.G. Courty, M. Kaufman, A.J. Clarke, Solid-solution strengthening in refractory high entropy alloys, *Acta Mater.* 175 (2019) 66–81.
- [66] Z. Li, et al., Interstitial atoms enable joint twinning and transformation induced plasticity in strong and ductile high-entropy alloys, *Sci. Rep.* 7 (1) (2017) 40704.
- [67] T. Yang, et al., Control of nanoscale precipitation and elimination of intermediate-temperature embrittlement in multicomponent high-entropy alloys, *Acta Mater.* 189 (2020) 47–59.
- [68] M.Z. Ahmed, et al., Influence of process parameters on microstructure evolution during hot deformation of a eutectic high-entropy alloy (EHEA), *Metall. Mater. Trans. P* 51 (2020) 6406–6420.
- [69] B. Cao, et al., Cocktail effects in understanding the stability and properties of face-centered-cubic high-entropy alloys at ambient and cryogenic temperatures, *Scripta Mater.* 187 (2020) 250–255.
- [70] G. Dwivedi, et al., Role of electron-magnon interaction in non-Fermi liquid behavior of SrRuO₃, *J. Phys. Condens. Matter* 31 (12) (2019) 125602.
- [71] A.M. Hofmeister, J. Dong, J.M. Branlund, Thermal diffusivity of electrical insulators at high temperatures: evidence for diffusion of bulk phonon-polaritons at infrared frequencies augmenting phonon heat conduction, *J. Appl. Phys.* 115 (16) (2014).
- [72] S. Uporov, et al., A single-phase ScTiZrHf high-entropy alloy with thermally stable hexagonal close-packed structure, *Intermetallics* 122 (2020) 106802.

- [73] Z. Sun, et al., Thermal physical properties of high entropy alloy Al0.3CoCrFeNi at elevated temperatures, *J. Alloys Compd.* 901 (2022) 163554.
- [74] H.-P. Chou, et al., Microstructure, thermophysical and electrical properties in AlxCrFeNi ($0 \leq x \leq 2$) high-entropy alloys, *Mater. Sci. Eng., B* 163 (3) (2009) 184–189.
- [75] M.-H. Tsai, Physical properties of high entropy alloys, *Entropy* 15 (12) (2013) 5338–5345.
- [76] A. Inoue, Stabilization of metallic supercooled liquid and bulk amorphous alloys, *Acta Mater.* 48 (1) (2000) 279–306.
- [77] C.-L. Lu, et al., Thermal expansion and enhanced heat transfer in high-entropy alloys, *J. Appl. Crystallogr.* 46 (3) (2013) 736–739.
- [78] S.K. Dewangan, et al., Enhancing the oxidation resistance of nanocrystalline high-entropy AlCuCrFeMn alloys by the addition of tungsten, *J. Mater. Res. Technol.* 21 (2022) 4960–4968.
- [79] Z. Fan, et al., Thermoelectric high-entropy alloys with low lattice thermal conductivity, *RSC Adv.* 6 (57) (2016) 52164–52170.
- [80] S. Huang, et al., Thermal expansion, elastic and magnetic properties of FeCoNiCu-based high-entropy alloys using first-principle theory, *Jom* 69 (2017) 2107–2112.
- [81] M.A. Al Hasan, et al., Effects of aluminum content on thermoelectric performance of AlxCrFeNi high-entropy alloys, *J. Alloys Compd.* 883 (2021) 160811.
- [82] E. Enriquez, et al., New strategy to mitigate urban heat island effect: energy saving by combining high albedo and low thermal diffusivity in glass ceramic materials, *Sol. Energy* 149 (2017) 114–124.
- [83] M. Farooq, et al., Cd-doping a facile approach for better thermoelectric transport properties of BiCuSeO oxyseLENides, *RSC Adv.* 6 (40) (2016) 33789–33797.
- [84] J. Hou, et al., Ultrafine-grained dual phase Al0.45CoCrFeNi high-entropy alloys, *Mater. Des.* 180 (2019) 107910.
- [85] S. Shafee, et al., High-entropy alloys as high-temperature thermoelectric materials, *J. Appl. Phys.* 118 (18) (2015).
- [86] S. Zhao, Role of chemical disorder and local ordering on defect evolution in high-entropy alloys, *Phys. Rev. Mater.* 5 (10) (2021) 103604.
- [87] Y. Yu, et al., Simultaneous optimization of electrical and thermal transport properties of Bi0.5Sb1.5Te3 thermoelectric alloy by twin boundary engineering, *Nano Energy* 37 (2017) 203–213.
- [88] S.A.A. Shams, et al., Effect of grain size on the low-cycle fatigue behavior of carbon-containing high-entropy alloys, *Mater. Sci. Eng., A* 810 (2021) 140985.
- [89] Z. Wang, I. Baker, Interstitial strengthening of a fcc FeNiMnAlCr high entropy alloy, *Mater. Lett.* 180 (2016) 153–156.
- [90] D. Yang, et al., A novel FeCrNiAlTi-based high entropy alloy strengthened by refined grains, *J. Alloys Compd.* 823 (2020) 153729.
- [91] W. Lu, et al., Advancing strength and counteracting embrittlement by displacive transformation in heterogeneous high-entropy alloys containing sigma phase, *Acta Mater.* 246 (2023) 118717.
- [92] M.R. Zamani, et al., Grain growth in high-entropy alloys (HEAs): a review, *High Entropy Alloys & Materials* (2022) 1–35.
- [93] L. Lin, et al., Microstructure stability and its influence on the mechanical properties of CrMnFeCoNiAl 0.25 high entropy alloy, *Met. Mater. Int.* 26 (2020) 1192–1199.
- [94] L. Zhang, et al., A ductile high entropy alloy strengthened by nano sigma phase, *Intermetallics* 122 (2020) 106813.
- [95] G. Qin, et al., Improvement of microstructure and mechanical properties of CoCrCuFeNi high-entropy alloys by V addition, *J. Mater. Eng. Perform.* 28 (2019) 1049–1056.
- [96] U. Hecht, et al., The BCC-FCC phase transformation pathways and crystal orientation relationships in dual phase materials from Al-(Co)-Cr-Fe-Ni alloys, *Front. Mater.* 7 (2020) 287.
- [97] J. Ding, et al., Tunable stacking fault energies by tailoring local chemical order in CrCoNi medium-entropy alloys, *Proc. Natl. Acad. Sci. USA* 115 (36) (2018) 8919–8924.
- [98] S. Liu, et al., Stacking fault energy of face-centered-cubic high entropy alloys, *Intermetallics* 93 (2018) 269–273.
- [99] E.P. George, W. Curtin, C.C. Tasan, High entropy alloys: a focused review of mechanical properties and deformation mechanisms, *Acta Mater.* 188 (2020) 435–474.
- [100] G. Meng, et al., Reinforcement and substrate interaction in laser surface forming of AlCoCrCuFeNi particle reinforced AZ91D matrix composites, *J. Alloys Compd.* 672 (2016) 660–667.
- [101] K. Ming, X. Bi, J. Wang, Microstructures and deformation mechanisms of Cr26Mn20Fe20Co20Ni14 alloys, *Mater. Char.* 134 (2017) 194–201.
- [102] C.Z. Hargather, Efficient first-principles methodologies for calculating Stacking Fault energy in FCC and BCC high-entropy alloys, *High-Entropy Materials: Theory, Experiments, and Applications* (2021) 315–354.
- [103] D. Thoma, *Intermetallics: laves phases*. Encyclopedia of Materials, Sci. Technol. (2001) 4205–4213.
- [104] G. Qin, et al., Microstructures and mechanical properties of Nb-alloyed CoCrCuFeNi high-entropy alloys, *J. Mater. Sci. Technol.* 34 (2) (2018) 365–369.
- [105] Y. Zhang, et al., Improved corrosion resistance of super austenite stainless steel by B-induced nucleation of Laves phase, *Corrosion Sci.* 213 (2023) 110974.
- [106] L. Fang, et al., Effect of Cr content on microstructure characteristics and mechanical properties of ZrNbTaHf0.2Crx refractory high entropy alloy, *J. Alloys Compd.* 924 (2022) 166593.
- [107] N. Razumov, et al., Refractory crmonbw high-entropy alloy manufactured by mechanical alloying and spark plasma sintering: evolution of microstructure and properties, *Materials* 14 (3) (2021) 621.
- [108] S. Mishra, A. Bajpai, K. Biswas, TiVCrNiZrFex High entropy alloy: phase evolution, magnetic and mechanical properties, *J. Alloys Compd.* 871 (2021) 159572.
- [109] B. Xin, et al., Enhancing mechanical properties of the boron doped Al0.2Co1.5CrFeNi1.5Ti0.5 high entropy alloy via tuning composition and microstructure, *J. Alloys Compd.* 896 (2022) 162852.
- [110] Y. Dong, et al., Effects of electro-negativity on the stability of topologically close-packed phase in high entropy alloys, *Intermetallics* 52 (2014) 105–109.
- [111] K. Park, P. Withey, Observation of the dissolution of topologically close packed phases by an additional heat treatment in third generation nickel-based single crystal superalloy turbine blades, *Adv. Eng. Mater.* 20 (7) (2018) 1700987.
- [112] J. Li, et al., The precipitation and effect of topologically close-packed phases in Ni-based single crystal superalloys, *J. Mater. Sci. Technol.* 173 (2023) 149–169, 20 February 2024.
- [113] Research, Laves Image, 2023 [cited 2023 15/09/2023]; Available from: <https://www.bing.com/search?pglt=41&q=image+of+Laves+phase&cvid=ff73dcfab514244af058161cbc9f7&qs=edge..69i57j014.13222j0j1&FORM=ANNTA1&PC=U531>.
- [114] Research, TCP, 2023 [cited 2023 15/09/2023]; Available from: <https://www.bing.com/search?q=image+of+Topological+close+packed&qs=n&form=QBRE&sp=1&glq=2&lq=0&pq=image+of+topological+close+packed+sc=8-34&sk=&cvid=364ECC2048264B34958B31CDC451CE73&ghsh=0&ghacc=0&ghpl=-->.
- [115] M.C. Oh, et al., Controlled valence electron concentration approach to tailor the microstructure and phase stability of an entropy-enhanced AlCoCrFeNi alloy, *Metall. Mater. Trans.* 53 (5) (2022) 1831–1844.
- [116] A. Sharma, H. Lee, B. Ahn, Effect of additive elements ($x = \text{Cr}, \text{Mn}, \text{Zn}, \text{Sn}$) on the phase evolution and thermodynamic complexity of AlCuSiFe-X high entropy alloys fabricated via powder metallurgy, *Met. Mater. Int.* (2022) 1–9.
- [117] A. Sharma, H. Lee, B. Ahn, Tailoring compressive strength and absorption energy of lightweight multi-phase AlCuSiFeX ($X = \text{Cr}, \text{Mn}, \text{Zn}, \text{Sn}$) high-entropy alloys processed via powder metallurgy, *Materials* 14 (17) (2021) 4945.
- [118] M.C. Oh, et al., Phase separation and mechanical behavior of AlCoCrFeNi-X ($X = \text{Cu}, \text{Mn}, \text{Ti}$) high entropy alloys processed via powder metallurgy, *Intermetallics* 139 (2021) 107369.
- [119] M.J. Chae, et al., Effect of light ($X = \text{Mg}, \text{Si}$) and heavy ($X = \text{Zn}$) metals on the microstructural evolution and densification of AlCuFeMnTi-X high-entropy alloy processed by advanced powder metallurgy, *Powder Metall.* 64 (3) (2021) 228–234.
- [120] P. Sengupta, I. Manna, Advanced high-temperature structural materials in petrochemical, metallurgical, power, and aerospace sectors—an overview, *Future landscape of structural materials in India* (2022) 79–131.
- [121] Research, Jet Engines, 2023 [cited 2023 23/09/2023]; Available from: <https://www.bing.com/images/search?view=detailV2&ccid=bYQwfGry&id=EC1832E4AF5756BD2095EE20C9397DF669E99688&thid=OIP.bYQwfGryAURF95CfS-6agHaE3&mediaurl=https%3A%2F%2Fwww.researchgate.net>.
- [122] K.R. Lim, et al., Dual-phase high-entropy alloys for high-temperature structural applications, *J. Alloys Compd.* 728 (2017) 1235–1238.
- [123] G. Popescu, et al., New TiZrNbTaFe high entropy alloy used for medical applications, in: IOP Conference Series: Materials Science and Engineering, IOP Publishing, 2018.
- [124] T.C. Dzogbewu, D. de Beer, Powder bed fusion of multimaterials, *Journal of Manufacturing and Materials Processing* 7 (1) (2023) 15.
- [125] M. Masadeh, et al., Antibacterial activity of statins: a comparative study of atorvastatin, simvastatin, and rosuvastatin, *Ann. Clin. Microbiol. Antimicrob.* 11 (1) (2012) 1–5.
- [126] J. Bray, et al., Influence of pharmacogenetics on response and toxicity in breast cancer patients treated with doxorubicin and cyclophosphamide, *Br. J. Cancer* 102 (6) (2010) 1003–1009.
- [127] C.P. Popolin, et al., Cytotoxicity and anti-tumor effects of new ruthenium complexes on triple negative breast cancer cells, *PLoS One* 12 (9) (2017), e0183275.
- [128] T.A. Batchelor, et al., High-entropy alloys as a discovery platform for electrocatalysis, *Joule* 3 (3) (2019) 834–845.
- [129] T. Löffler, et al., Discovery of a multinary noble metal-free oxygen reduction catalyst, *Adv. Energy Mater.* 8 (34) (2018) 1802269.
- [130] M. Sahlberg, et al., Superior hydrogen storage in high entropy alloys, *Sci. Rep.* 6 (1) (2016) 36770.
- [131] S. Xia, M. Gao, Y. Zhang, Abnormal temperature dependence of impact toughness in AlxCrFeNi system high entropy alloys, *Mater. Chem. Phys.* 210 (2018) 213–221.
- [132] Y. Tang, D. Li, Dynamic response of high-entropy alloys to ballistic impact, *Sci. Adv.* 8 (31) (2022) eabp9096.
- [133] S. Son, et al., Superior antifouling properties of a CoCrFeMnNi high-entropy alloy, *Mater. Lett.* 300 (2021) 130130.
- [134] M. Zhang, et al., Anticorrosive superhydrophobic high-entropy alloy coating on 3D iron foam for efficient oil/water separation, *Surf. Coatings. Technol.* 468 (2023) 129756.
- [135] W. Savage, *Joining of Advanced Materials*, Elsevier, 2013.
- [136] S. Zhao, et al., Pseudo-quinary Ti20Zr20HF20Be20 (Cu20-xNix) high entropy bulk metallic glasses with large glass forming ability, *Mater. Des.* 87 (2015) 625–631.
- [137] W. Keller, F properties, at temperatures above 1000 °C, of materials WHICH melt below 1500 °C a metallic materials 1 native defects and stoichiometry in GaAlAs gm blom (philips labs, briarcliff manor, New York 10510 US) J of crystal growth, Bibliography on the High Temperature Chemistry and Physics of Materials 36 (1) (1976) 125–137, 1976. 20(3): pp. 237–246.

- [138] A. Fornalczyk, Industrial catalysts as a source of valuable metals, *Journal of Achievements in Materials and Manufacturing Engineering* 55 (2) (2012) 864–869.
- [139] T.B. Holland, U. Anselmi-Tamburini, A.K. Mukherjee, Electric fields and the future of scalability in spark plasma sintering, *Scripta Mater.* 69 (2) (2013) 117–121.
- [140] C. Ujah, et al., Influence of CNTs addition on the mechanical, microstructural, and corrosion properties of Al alloy using spark plasma sintering technique, *Int. J. Adv. Des. Manuf. Technol.* 106 (2020) 2961–2969.
- [141] S.K. Dewangan, et al., Review on applications of artificial neural networks to develop high entropy alloys: a state-of-the-art technique, *Mater. Today Commun.* (2023) 107298.